In-Band Full-duplex Residual Self-interference Approximation in Multi-tap Delay Fading Channels

Ayman T. Abusabah [†‡], Luis Irio[‡], and Rodolfo Oliveira[†‡]
[†]Departamento de Engenharia Electrotécnica, Faculdade de Ciências e Tecnologia, FCT,
Universidade Nova de Lisboa, 2829-516 Caparica, Portugal
[‡]IT, Instituto de Telecomunicações, Portugal
Emails: a.sabah@campus.fct.unl.pt, l.irio@campus.fct.unl.pt, rado@fct.unl.pt

***Abstract*—Residual self-interference (SI) is primarily a key challenge when designing In-Band Full-duplex (IBFDX) wireless systems. Channel estimation errors are one of the major causes of the residual SI. The SI channel is composed by multiple fading taps which makes the characterization of the residual SI more challenging as multiple copies of the transmitted signal, with variable delays and gains, are eventually aggregated at the receiver. In this paper, we derive an approximation for the distribution of the residual SI power in multi-tap delay fading channels. In particular, we show that under specific conditions the multi-tap fading channel can be represented by a summation of non-identical independent gamma distributions. In a further step, we approximate the summation of the gamma distributions using the Welch-Satterthwaite equation, obtaining a closed form expression for the distribution of the residual SI power. The accuracy of the theoretical approach is evaluated through simulation results. The similarity comparison between simulated data and the proposed model indicates a high accuracy of the adopted approximation when considering low fading uncertainty associated to the taps and low estimation errors. On the other hand, the accuracy of the approximation slightly decreases for higher uncertainty fading scenarios and for higher estimation errors. However, as a final remark, we highlight that the results computed with the model are close to the simulated ones and for most of the applications the model's error can be negligible.**

Keywords: In-Band Full-duplex Wireless Communications, Residual Self-interference, Stochastic Modeling, Performance Analysis.

I. INTRODUCTION

In In-Band Full-Duplex (IBFDX) communications, the nodes can transmit and receive the signals simultaneously on the same frequency [1]. Compared with half-duplex communication systems, where the resources are divided between transmission and reception, the capacity of the communication link can be doubled [2].

The key challenge when designing the IBFDX system is to reduce the amount of residual self-interference (SI). The residual SI is defined as the amount of remaining signal after the cancellation of the SI signal. Most of times, the transmitted signal is propagated over multiple paths, so, multiple copies, with random gains and phases, are combined at the receiver. The SI can be mitigated by a combination of passive and active methods [3]. Passive methods use antenna design, cross-polarization or shielding to achieve a significant amount of signal suppression [4]. On the other hand, active methods exploit the knowledge of the SI signal to decode the signal received from other transmitter [5]. Apart from hardware impairments, the amount of the residual SI power is mainly related to the accuracy of the estimated channel parameters. The SI channel must be estimated to cancel the SI contributions propagated in non Line-of-Sight, due to multiple signal reflections. Consequently, inaccurate channel estimates will result in an increased level of SI and this is the main reason why active methods are unable to eliminate the SI signal totally. Therefore, subtracting an inverted copy of the transmitted signal at the receiver is not sufficient to suppress the residual SI perfectly.

To minimize the amount of the residual SI, it is important to characterize its power under the effects of the propagation channel. This knowledge is particularly useful to design efficient digital cancellation-domain techniques, where more appropriate estimation techniques can be used depending on the distribution of the residual SI power.

A. Related Work

In IBFDX communications, the transmitter's signal must be reduced to an acceptable level at the receiver located at the same node. Any residual SI will increase the received noise floor, thus reducing the capacity of the receiver. Usually, in a mobile wireless communication system a device transmits at approximately 21 dBm and the base station's noise floor is approximately -94 dBm [6]. Assuming a typical isolation of 15 dB due to the physical separation between the receiving and transmitting antennas, the received signal is approximately 102 dB above the noise floor, which gives the amount of SI that must be suppressed to achieve the same signal-to-noise ratio (SNR) of a half-duplex system.

The success of IBFDX communications depends on the efficiency of SI Cancellation (SIC) techniques. Multiple SIC techniques have been presented in the last years [7]–[9]. To effectively reduce the amount of SI to negligible levels more efficient active cancellation techniques are required. Active cancellation encompasses analog and digital-domain techniques [10]. Due to the proximity of the transmitting and receiving antennas, the SI signal is too strong. This causes a high probability of saturation of the radio-frequency front-end and analog-to-digital converters, which may invalidate the digital processing. Thus, the SI signal has to be cancelled in

the analogue domain first. Most of the full-duplex systems described in the literature perform these cancellation steps sequentially, but recent works already propose a simultaneous analog/digital cancellation design [11], [12], where the goal is to optimize the overall analog/digital canceler to achieve maximum cancellation. The SI channel must be estimated to cancel the SI contributions propagated in non-direct path (i.e. multi-path components due to reflection). This is the main reason for the adoption of digital cancellation. Inaccurate channel estimates will result in an increased level of SI. Due to the channel's time-varying nature, it is important to capture different channel's uncertainty levels and their impact in the residual SI power, which can be used to improve the adaptive digital cancellation.

Despite of its importance, the characterization of the stochastic properties of the residual SI has received limited attention due to the difficulty of the mathematical modeling process [13]–[15]. In [13], the amount of cancellation and the strength of residual SI were computed considering a single-tap delay channel. The authors adopted a narrow-band signal model to characterize the residual SI power, i.e., it is assumed that the signal time is less than the coherence time of the channel. The similarity of the residual SI distribution with known distributions was analysed in [14] for a single-tap delay channel. In [15], the distribution of the residual SI power was also characterized for a single-tap delay channel. In particular, the proposed modeling methodology assumes a narrow-band transmitting signal and a sampling rate of several orders of magnitude higher. The estimation of the channel with a single tap delay was studied in [16].

B. Contributions

Motivated by the importance of analysing the residual SI power in real and practical channel scenarios, this work derives the distribution of residual SI power in a multi-tap fading channel for IBFDX systems. To the best of the authors' knowledge, this is the first work considering the distribution of the residual SI power in multi-tap fading channel.

First, the residual SI power is mathematically formulated when considering Rician fading independent multi-taps. During the derivation, the aggregation of independent Rician fading taps is approximated by a Gamma distribution utilizing the Welch-Satterthwaite equation. As a result, the distribution of residual SI power can be computed by solving a classical product distribution. The final expression is provided and evaluated through simulation. To examine the accuracy of the theoretical analysis, the numerical results are compared with Monte Carlo simulation results. The results demonstrate that the proposed approximation is precise when the uncertainty of the taps' parameters and estimation errors, i.e., phase and gain, is relatively small. However, the accuracy of the approximation decreases when the uncertainty level of the taps and estimation errors is significantly high.

The rest of this paper is organized as follows. In Section II, we present the architecture and mathematical formulation of multi-tap delay fading channel in IBDFDX systems. In Section III, we derive an approximated model for the residual SI power utilizing Welch-Satterthwaite approximation. We validate the derivations and approximations through simulation results presented in Section IV. Finally, Section V concludes the paper.

II. SYSTEM MODEL

A. In-Band Full Duplex Canceller

In this paper, we consider a full-duplex scheme adopting an active analog canceler [13] that reduces the SI at the angular carrier frequency $\omega_c = 2\pi f_c$. The system model is depicted in Fig. 1. Multi-tap delay fading channel with I taps is considered. Thus, multiple shifted versions of the SI signal $x_s(t)$ with different amplitudes are observed at the receiver side. Each tap, i.e., i^{th} tap, is characterized by a delay τ_i and gain h_i. To obtain the residual SI signal $y_{res}(t)$, the estimated delay $\hat{\tau}_i$ and estimated gain $\hat{h}_i$, for each tap, have to be injected in the cancellation process [13].

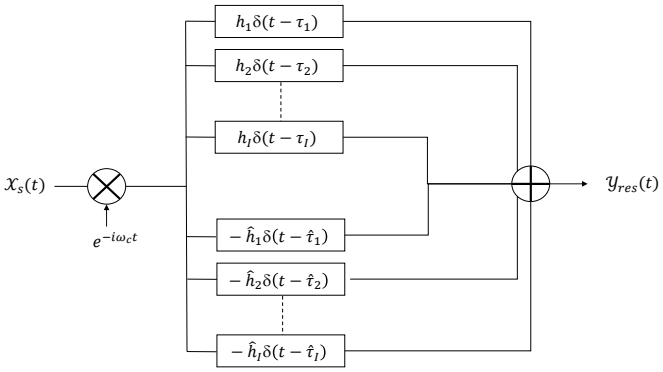

Fig. 1. Block diagram of multi-tap delay fading channel canceller in IBFDX system.

B. Residual Self-Interference Power

Generally, for I-taps and according to Fig. 1, the residual SI, $y_{res}(t)$, can be written as follows

$$y_{res}(t) = \sum_{i=1}^{I} h_i x_s(t-\tau_i) e^{j\omega_c(t-\tau_i)} - \hat{h}_i x_s(t-\hat{\tau}_i) e^{j\omega_c(t-\hat{\tau}_i)}, \tag{1}$$

where channel gains are independent and complex random variables, i.e., $h_i = h_{r_i} + j h_{j_i}$. The estimated gain is given by $\hat{h}_i = \epsilon_i h_i$, where $(1-\epsilon_i)$ is the gain estimation error of the i^{th} tap, i.e., for $\epsilon_i = 1$ the channel's tap is perfectly estimated and for $\epsilon_i = 0$ the estimation is totally corrupted. We also assume that $x_s(t)$ is a circularly-symmetric complex random signal given by $x_s(t) = x_r(t) + j x_j(t)$. The circularly-symmetric complex distribution is considered because it can effectively represent Orthogonal Frequency-Division Multiplexing systems with high number of carriers.

Considering a narrow band channel, i.e., $x_s(t-\tau_i) = x_s(t-\hat{\tau}_i)$, then (1) can be represented as follows

$$y_{res}(t) = x_s(t)\sum_{i=1}^{I} h_i c_i, \tag{2}$$

where $c_i = \left(e^{j\omega_c(t-\tau_i)} - \epsilon_i\ e^{j\omega_c(t-\hat{\tau}_i)}\right)$ is a constant. Since the terms $x_s(t)$, h_i, and c_i are complex, and considering that the channel gains of the taps are independent, then, the residual SI power can be expressed as

$$P_{y_{res}} = \left(X_r^2 + X_j^2\right)\sum_{i=1}^{I}\left(H_{r_i}^2 + H_{j_i}^2\right)C_i, \tag{3}$$

where $C_i = \left(1+{\epsilon_i}^2 - 2\epsilon_i\cos\left(\phi_i\right)\right) = \left((\Re(c_i))^2 + (\Im(c_i))^2\right)$ is also a constant which represents the power of c_i. The phase estimation error of the i^{th} tap is given by $\phi_i = \omega_c(\tau_i - \hat{\tau}_i)$.

According to (3), the residual SI power represents the power of the SI signal multiplied with the power of the composed taps. Obviously, the power of the fading taps, and thus the power of the residual SI, is a function of the gain and phase estimation errors. Specifically, when $\phi_i = 0$ and $\epsilon_i = 1$, then, $C_i = 0$ and therefore the additive power of the i^{th} tap is null. On the other hand, when $\phi_i = \pi$ and $\epsilon_i = 1$, then, $C_i = 4$ and therefore the additive power is maximum.

III. CHARACTERIZATION OF RESIDUAL SELF-INTERFERENCE POWER

This section considers the required steps to derive the distribution of the residual SI power, denoted by $P_{y_{res}}$. In fact, (3) can be seen as a product of two random variables, $X = X_r^2 + X_j^2$ and $H = \sum_{i=1}^{I}\left(H_{r_i}^2 + H_{j_i}^2\right)C_i$.

A. Characterization of Random Variable X

As mentioned earlier, the signal $x_s(t)$ is a circularly-symmetric complex signal, with $X_r \sim \mathcal{N}(0,\, \sigma_x^2)$ and $X_j \sim \mathcal{N}(0,\, \sigma_x^2)$. Departing from (3), X_r^2 and X_j^2 follow a scaled Chi-squared distribution with $k = 1$ degrees of freedom denoted by χ_1^2 and may be written as follows

$$X_r^2 \sim \sigma_x^2\chi_1^2,\ \ X_j^2 \sim \sigma_x^2\chi_1^2. \tag{4}$$

By definition, if $Q \sim \chi_k^2$ and v is a positive constant, then $vQ \sim Gamma(k/2, 2v)$. Consequently,

$$X_r^2 \sim Gamma(1/2, 2\sigma_x^2),\ \ X_j^2 \sim Gamma(1/2, 2\sigma_x^2). \tag{5}$$

Finally, the sum of two gamma random variables, holding different shape parameters and the same scale parameter, results another gamma distribution, i.e., $Gamma(k_1,\theta) + Gamma(k_2,\theta) = Gamma(k1+k2,\theta)$, thus,

$$X = X_r^2 + X_j^2 \sim Gamma(1, 2\sigma_x^2). \tag{6}$$

B. Characterization of Random Variable H

The random variable H represents a composition of I independent fading taps. In this work, the gain of each tap is modeled as a Rician fading channel. To find the distribution of H, we firstly consider the distribution of a single Rician channel. A Rician fading channel can be described by two parameters: K and Ω. K is the ratio between the power in the direct path and the power in the other paths. Ω is the total power from both paths. Then, the received signal amplitude, of the i^{th} tap, is Rician distributed with parameters $\mu_{h_i}^2 = \frac{K_i\Omega_i}{1+K_i}$ and $\sigma_{h_i}^2 = \frac{\Omega_i}{2(1+K_i)}$. $K_{dB} = 10\log_{10}(K)$ is the decibels representation of K.

If the i^{th} tap is a Rician, then, $H_{r_i} \sim \mathcal{N}(\mu_{h_i}\cos(\vartheta_i),\, \sigma_{h_i}^2)$ and $H_{j_i} \sim \mathcal{N}(\mu_{h_i}\sin(\vartheta_i),\, \sigma_{h_i}^2)$. Consequently, the term $(1/\sigma_{h_i}^2)(H_{r_i}^2 + H_{j_i}^2)$ follows a non-central Chi-squared distribution with $k = 2$ degrees of freedom and non-centrality parameter $\mu_{h_i}^2/\sigma_{h_i}^2$. Using the method of moments, a gamma approximation can be provided and the shape and scale parameters, k_{h_i} and θ_{h_i} respectively, are found to be

$$\begin{aligned} k_{h_i} &= \frac{(\mu_{h_i}^2 + 2\sigma_{h_i}^2)^2}{4\sigma_{h_i}^2(\mu_{h_i}^2 + \sigma_{h_i}^2)}, \\ \theta_{h_i} &= \frac{4(\mu_{h_i}^2 + \sigma_{h_i}^2)}{(\mu_{h_i}^2 + 2\sigma_{h_i}^2)}. \end{aligned} \tag{7}$$

Since C_i is a constant, the term $\left(H_{r_i}^2 + H_{j_i}^2\right)C_i$ can be written as follows

$$\left(H_{r_i}^2 + H_{j_i}^2\right)C_i \sim Gamma(k_{h_i}, \theta_{h_i}\sigma_{h_i}^2 C_i). \tag{8}$$

Consequently, the distribution of the random variable H represents a summation of independent gamma distributions holding different shape and scale parameters.

C. Welch-Satterthwaite Approximation

As seen before, the summation of gamma distributions holding same scale parameters has a closed form solution. However, there is no obvious solution when the scale parameters are different. In this work, we use the Welch-Satterthwaite method to approximate H. The original Welch-Satterthwaite approximation was for linear combinations of independent Chi-square random variables. However, their basic idea easily extends to sums of independent gamma random variables [17], [18].

Let $H_1, ..., H_I$ be independent gamma random variables with $H_i \sim Gamma(k_i, \theta_i)$, and $H = H_1 + ... + H_I$ be their sum, then

$$H \sim Gamma(k_{eq}, \theta_{eq}), \tag{9}$$

where k_{eq} and θ_{eq} are the equivalent shape and scale parameters, respectively, and given by

$$\begin{aligned} k_{eq} &= \frac{(k_1\theta_1 + ... + k_I\theta_I)^2}{k_1\theta_1^2 + ... + k_I\theta_I^2}, \\ \theta_{eq} &= \frac{k_1\theta_1^2 + ... + k_I\theta_I^2}{k_1\theta_1 + ... + k_I\theta_I}. \end{aligned} \tag{10}$$

Substituting (7) in (10) leads to

$$k_{eq} = \frac{(\sum_{i=1}^{I} k_{h_i}\theta_{h_i}\sigma_{h_i}^2 C_i)^2}{\sum_{i=1}^{I} k_{h_i}(\theta_{h_i}\sigma_{h_i}^2 C_i)^2}, \quad \forall i,$$
$$\theta_{eq} = \frac{\sum_{i=1}^{I} k_{h_i}(\theta_{h_i}\sigma_{h_i}^2 C_i)^2}{\sum_{i=1}^{I} k_{h_i}(\theta_{h_i}\sigma_{h_i}^2 C_i)}, \quad \forall i. \tag{11}$$

D. Characterization of Random Variable $P_{y_{res}}$

The random variable X is independent of the random variable H. Thus, the probability density function of $P_{y_{res}}$ is given by the classical product density function between H and X as follows

$$f_{P_{y_{res}}}(z) = \int_{-\infty}^{\infty} f_X(x) f_H(z/x) \frac{1}{\mid x \mid} dx. \tag{12}$$

Both random variables X and H follow a gamma distribution and (12) can be solved by replacing $f_X(x)$ and $f_H(z/x)$ by (6) and (9), respectively, as shown in [15]. After solving the integral, the probability density function (PDF) and the cumulative distribution function (CDF) of the residual SI power are given by (13) and (14), respectively

$$f_{P_{y_{res}}}(z) = \frac{2^{\frac{1-k_{eq}}{2}} \sigma_x^{-k_{eq}-1} \theta_{eq}^{-k_{eq}}}{\Gamma(k_{eq})} \times (\theta_{eq}/z)^{\frac{k_{eq}-1}{2}} z^{k_{eq}-1} K_{(k_{eq}-1)}\left(\sqrt{\frac{2z}{\sigma_x^2\theta_{eq}}}\right), \tag{13}$$

$$F_{P_{y_{res}}}(z) = 1 - \left(\frac{2^{\frac{1-k_{eq}}{2}} (\theta_{eq} z)^{\frac{k_{eq}}{2}} K_{k_{eq}}\left(\sqrt{\frac{2z}{\sigma_x^2\theta_{eq}}}\right)}{(\sigma_x\theta_{eq})^{k_{eq}}\Gamma(k_{eq})} \right), \tag{14}$$

where $K_{(k_{eq})}(.)$ denotes the modified Bessel function of the second kind. $\Gamma(.)$ represents the complete Gamma function.

IV. PERFORMANCE ANALYSIS

A. Evaluation Methodology

The evaluation of the model presented in Section III, done through the comparison of Monte Carlo simulations w numerical results. Regarding the simulation, the system des in Fig. 1 is adopted. The carrier frequency is adjusted to f_c = GHz. The values of X_r and X_j are sampled from Norr distributions with $\sigma_x^2 = \frac{1}{2}$. The gains of the taps are assumec be time-variant, so, H_{r_i} and H_{j_i} are sampled from independ Rician distributions. The total power is set to 10 mW for e tap, i.e., $\Omega_i = 10$ mW, $\forall i$.

The accuracy of the Welch-Satterthwaite approximation evaluated by considering two scenarios:

- S_1 - when the uncertainty of Rician fading taps and chan estimation errors is relatively small, by adopting values in Table I;
- S_2 - when the uncertainty is significantly high, by adopting the values in Table II.

TABLE I
VARIATION IN TAPS PARAMETERS AND ESTIMATION ERRORS ADOPTED IN THE SCENARIO S_1.

I	K_{dB}	μ_h	σ_h^2	ϑ°	ϵ	ϕ°	k_{eq}	θ_{eq}
1	9.08	2.98	0.55	45	1.00	60	4.8	2.0
2	9.17	2.98	0.54	60	0.90	30	7.1	1.7
3	9.00	2.98	0.56	70	0.80	20	8.5	1.6
4	9.35	3.00	0.52	50	0.77	40	12.5	1.4
5	9.84	3.01	0.47	30	0.89	35	16.3	1.3
6	10.60	3.03	0.40	40	0.86	45	22.0	1.2

TABLE II
VARIATION IN TAPS PARAMETERS AND ESTIMATION ERRORS ADOPTED IN THE SCENARIO S_2.

I	K_{dB}	μ_h	σ_h^2	ϑ°	ϵ	ϕ°	k_{eq}	θ_{eq}
1	12	3.00	0.3	20	0.9	60	8.5	1.0
2	-17	0.45	5.0	230	1.0	178	1.5	32.7
3	6	2.80	1.0	57	0.6	150	3.0	24.8
4	17	3.10	0.1	32	1.0	53	3.6	22.4
5	9.5	3.00	0.5	146	0.2	146	4.8	19.5
6	-6	1.40	4.0	254	1.0	234	5.7	22.3

B. Accuracy Assessment

First, we evaluate the CDF of the residual SI power considering the scenario S_1, when the dynamics of the taps and the estimation errors are relatively small (adopting the parameters in Table I). The theoretical results are compared with the simulation results in Fig. 2. The 'simulation' curves are obtained through Monte Carlo simulation while the 'theoretical' curves are obtained with the computation of (14). The results are obtained for $I = \{1, 2, 3, 4, 5, 6\}$ taps. As can be seen, the numerical results computed with (14) are close to the simulation results. Moreover, the additive effect of the taps can be observed, as the residual SI power increase with the number of taps (we highlight that this observation is only valid for the specific parameters considered in this scenario, since the addition of a new tap can also originate a null impact when it is perfectly canceled).

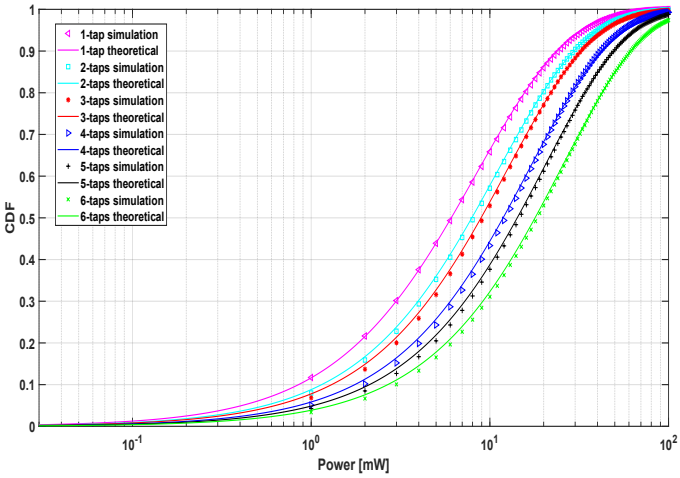

Fig. 2. CDF of residual SI power for $I = \{1, 2, 3, 4, 5, 6\}$ independent fading taps adopting Table I parameters.

Next we evaluate the proposed approach for the scenario S_2. The CDF of the residual SI power is evaluated considering the parameters in Table II. When the uncertainty associated to fading and estimation errors is high, the Welch-Satterthwaite approximation exhibits low accuracy at particular regions of the domain (low probability values), as depicted in Fig. 3. This is due to the fact that the higher uncertainty of the taps and estimation errors leads to a large variation in the scale parameters computed with (7) to obtain the different gamma distributions indicated in (8). As a result, the accuracy of the Welch-Satterthwaite approximation decreases as the resulting gamma distributions in (8) exhibit a higher dissimilarity of scale parameters. Anyway, we highlight that the results computed with the model are close to the simulated ones and for most of the applications the model's error can be negligible.

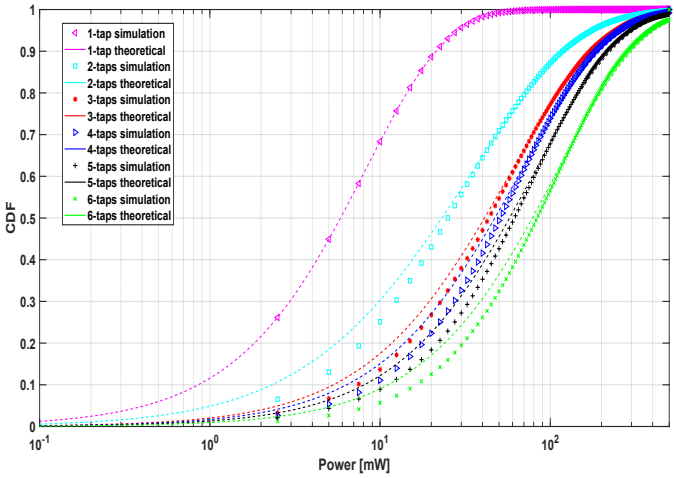

Fig. 3. CDF of residual SI power for $I = \{1, 2, 3, 4, 5, 6\}$ independent fading taps adopting Table II parameters.

V. Conclusions

In this paper, we have derived a closed-form approximation of PDF and CDF for the residual SI power in multi-tap delay fading channel. During the derivation, the fading channel was written as a summation of independent gamma random variables holding different scale parameters. The Welch-Satterthwaite equation was utilized to approximate the summation and the final expression of the residual SI power was obtained. The accuracy of the proposed approximation was assessed through Monte Carlo simulations. The reported results show high accuracy of the derivations when the randomness of the taps' parameters and estimation errors are small. However, the accuracy of the Welch-Satterthwaite approximation decreases, at specific regions of the domain, with the dissimilarity of the fading observed in the multiple taps. Although the accuracy of the proposed model is satisfactory for a large variety of parameters, the results indicate that better approximations have to be explored when considering a significant high randomness in the propagation channel, motivating further research efforts and the adoption of different approaches in the future.

The derived expressions of the residual SI power presented in this paper can be used to provide technical criteria for alleviating the residual SI in practical IBFDX communication systems. One of the practical applications is the compensation of the cancelation errors, i.e., the gain cancelation error $(1 - \epsilon)$ and the phase cancellation error (ϕ). Moreover, the obtained results may also be helpful for the academic community in general, to determine different aspects related to the performance analysis of IBFDX communications. For example, by using the residual SI power to derive the outage probability of a specific full-duplex system, the capacity of IBFDX communication systems can be achieved.

Acknowledgements

This work has received funding from the European Union's Horizon 2020 research and innovation programme under the Marie Skłodowska-Curie ETN TeamUp5G, grant agreement No. 813391, and partially supported by the projects CoSHARE (LISBOA-01-0145-FEDER0307095 - PTDC/EEI- TEL/30709/2017), InfoCent-IoT (POCI-01-0145-FEDER-030433), and UID/EEA/50008/2019.

References

[1] M. Heino, D. Korpi, T. Huusari, E. Antonio-Rodriguez, S. Venkatasubramanian, T. Riihonen, L. Anttila, C. Icheln, K. Haneda, R. Wichman, and M. Valkama. Recent advances in antenna design and interference cancellation algorithms for in-band full duplex relays. 53(5):91–101, May 2015.

[2] X. Xie and X. Zhang. Does full-duplex double the capacity of wireless networks? In *Proc. IEEE INFOCOM*, pages 253–261, Toronto, ON, Canada, Apr. 2014.

[3] A. Masmoudi and T. Le-Ngoc. A Maximum-Likelihood Channel Estimator for Self-Interference Cancelation in Full-Duplex Systems. 65(7):5122–5132, Jul. 2016.

[4] M. Duarte and A. Sabharwal. Full-duplex wireless communications using off-the-shelf radios: Feasibility and first results. In *2010 Conference Record of the Forty Fourth Asilomar Conference on Signals, Systems and Computers*, pages 1558–1562, Nov 2010.

[5] Mohammad Ali Khojastepour, Karthikeyan Sundaresan, Sampath Rangarajan, Xinyu Zhang, and Sanaz Barghi. The case for antenna cancellation for scalable full-duplex wireless communications. In *HotNets-X*, 2011.

[6] Small Cell Forum. Interference management in umts femtocells ("high-band"). https://scf.io/en/documents/003_Interference_management_in_UMTS_femtocells_high-band.php, Last accessed on 2020-02-10.

[7] Z. Zhang, X. Chai, K. Long, A. V. Vasilakos, and L. Hanzo. Full duplex techniques for 5g networks: self-interference cancellation, protocol design, and relay selection. *IEEE Communications Magazine*, 53(5):128–137, May 2015.

[8] M. Heino, D. Korpi, T. Huusari, E. Antonio-Rodriguez, S. Venkatasubramanian, T. Riihonen, L. Anttila, C. Icheln, K. Haneda, R. Wichman, and M. Valkama. Recent advances in antenna design and interference cancellation algorithms for in-band full duplex relays. *IEEE Communications Magazine*, 53(5):91–101, May 2015.

[9] B. Debaillie, D. van den Broek, C. LavÃÂn, B. van Liempd, E. A. M. Klumperink, C. Palacios, J. Craninckx, B. Nauta, and A. PÃrssinen. Analog/rf solutions enabling compact full-duplex radios. *IEEE Journal on Selected Areas in Communications*, 32(9):1662–1673, Sep. 2014.

[10] M. Duarte, C. Dick, and A. Sabharwal. Experiment-driven characterization of full-duplex wireless systems. *IEEE Transactions on Wireless Communications*, 11(12):4296–4307, December 2012.

[11] V. Tapio, H. Alves, and M. Juntti. Joint analog and digital self-interference cancellation and full-duplex system performance. In *2017 IEEE International Conference on Acoustics, Speech and Signal Processing (ICASSP)*, pages 6553–6557, March 2017.

[12] Y. Liu, P. Roblin, X. Quan, W. Pan, S. Shao, and Y. Tang. A full-duplex transceiver with two-stage analog cancellations for multipath self-interference. *IEEE Transactions on Microwave Theory and Techniques*, 65(12):5263–5273, Dec 2017.

[13] A. Sahai, G. Patel, C. Dick, and A. Sabharwal. On the impact of phase noise on active cancelation in wireless full-duplex. *IEEE Trans. on Veh. Technol.*, 62(9):4494–4510, Nov 2013.

[14] L. Irio and R. Oliveira. On the impact of fading on residual self-interference power of in-band full-duplex wireless systems. In *2018 14th International Wireless Communications Mobile Computing Conference (IWCMC)*, pages 142–146, June 2018.

[15] L. Irio and R. Oliveira. Distribution of the residual self-interference power in in-band full-duplex wireless systems. *IEEE Access*, 7:57516–57526, 2019.

[16] A. Quazi. An overview on the time delay estimate in active and passive systems for target localization. *IEEE Transactions on Acoustics, Speech, and Signal Processing*, 29(3):527–533, June 1981.

[17] F. E. Satterthwaite. An approximate distribution of estimates of variance components. *Biometrics Bulletin*, 2(6):110–114, 1946.

[18] B. L. Welch. The generalization of 'student's' problem when several different population variances are involved. *Biometrika*, 34(1/2):28–35, 1947.